TROPICAL SUBVISUAL CIRRUS AND CONTRAILS AT -85ºC

J. Michel Flores*[1], D. Baumgardner[1], G. Kok[2], G. Raga[1], and R. Hermann[3]
[1]Universidad Nacional Autónoma de México, Mexico City, Mexico
[2] Droplet Measurements Technologies, Boulder, Colorado
[3] Jet Propulsion Laboratory, Pasadena, California

1. INTRODUCTION

The impact of clouds is one of the biggest uncertainties in our present understanding of the radiation budget of the atmosphere. An understanding of the macro and microphysical properties of subvisual cirrus (SVC) is an even more complex problem given that they are invisible to the naked eye at most solar scattering angles and that they are usually located near the tropopause, a region difficult to reach in tropical regions with most research aircraft. SVC are defined as having an optical depth of 0.03 or less (Sassen and Cho 1992) and composed primarily of ice (WMO 1975). Few aircraft measurements have been made of SVC. Heymsfield [1986] reported in situ measurements of SVC over Kwajalein Atoll in the western Pacific Ocean at 16.2-16.7 kilometers and Pfister et al. [2001] made lidar observations in the central Pacific of SVC which at times were 18 km or higher. Jensen et al. [1996b] explored the formation processes of SVC and their persistence over the tropical tropopause.

In contrast to SVC, contrails are not a natural phenomenon as they're formed by anthropogenic injections from aircraft exhaust into the upper troposphere. With air traffic increasing about 5% a year (IPCC 1999) fuel emissions and contrail formation will have a greater effect in the environment, especially in the radiation energy field of the earth-atmosphere system. Contrails form when the relative humidity in the plume of exhaust gases mixing with the ambient air temporarily reaches or exceeds liquid saturation, liquid droplets form on cloud condensation nuclei and almost immediately freeze to ice particles (Schmidt 1941; Appleman 1953). There is also evidence

---

* *Corresponding author address:* J. Michel Flores, Centro de Ciancias de la Atmósfera, UNAM. Circuito Exterior s/n, Ciudad Universitaria, 04510 México City (D.F.), MEXICO.

that contrails may serve as seeds for the development of SVC.

The radiative effects of contrail and SVC depend on the number, size, shape of the particles and the ice water content. Here we explore the microphysical properties of aircraft contrails and SVC in the region of the tropical tropopause that was measured with a cloud aerosol and precipitation spectrometer (CAPS) during the Costa Rica Aura Validation Experiment (CR-AVE) in February 1 and 2, 2006. A comparison of the microphysical properties of the SVC and the contrails is made; we discuss the processes that could lead to mixed-phase cirrus and contrail at the tropical tropopause and the implications for heterogeneous chemical reactions, climate impact and interpretation of satellite measurements.

2. DESCRIPTION OF THE CAPS

The cloud, aerosol and precipitation spectrometer (CAPS), shown in figure 1, is a combination of three sensors for particle size and liquid water content (LWC) measurements.
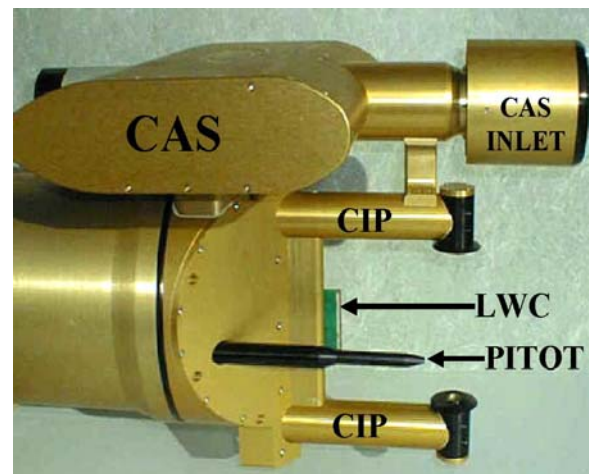

Figure 1. Photograph of the Cloud Aerosol and Precipitation Spectrometer (CAPS) showing the different components that measure liquid water content (LWC), airspeed (PITOT) and particle sizes from 0.5 to 50 μm (CAS) and 25 – 1600 μm.

The cloud and aerosol spectrometer (CAS) derives two size distributions from the light scattered by individual particles that pass through a focused beam from a diode laser (*Baumgardner et al.*, 2002). Two cones of light, 4 to 12° and 168° to 176°, are measured by separate detectors and the peak amplitudes are classified into size bins to create two frequency histograms, forward and backward, every second. Figure 2 is a schematic diagram of the optical configuration of the CAS. The relationship between scattered light intensity and detector voltage output is established with monodispersed polystyrene latex and crown glass beads of known size and refractive index. The peak amplitudes of the forward and backward scattering signals are recorded for individual particles. In addition, the time of arrival, i.e. the time between successive particles that arrive in the laser beam, is also recorded. The relationship between the forward
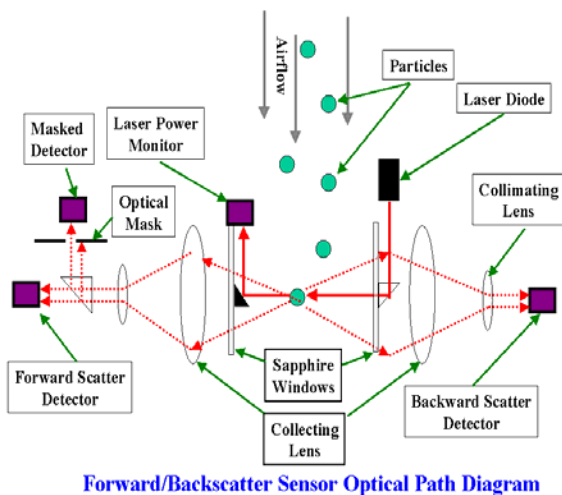

Forward/Backscatter Sensor Optical Path Diagram

Figure 2. The optical light collection configuration for CAS is shown in this schematic. The dotted lines illustrate the path of scattered ligh collected during a scatterign event.

and backward scattered light is a function of the particle size, refractive index and shape. This relationship is exploited in the CAS and used to derive either the particle's refractive index or shape from the ratio of forward and back scattered signals (*Baumgardner et al.*, 1996; *Baumgardner et al.*, 2005; *Chepfer et al.*, 2005).

Figure 3 illustrate the forward to back ratio (F2BR) as a function of size for particles with two refractive indices. For a specific size, in this example, the particle composition could be derived from the F2BR, i.e. water (1.33) or dry

sea salt (1.54). The F2BR is even more sensitive to the particle shape, as illustrated in Figure 4 where the F2BR is plotted for three diameters as a function of the aspect ratio of the particle, assuming these are oblate (aspect ratio < 1) or prolate (aspect ratio > 1) spheroids. These F2BRs were calculated using T-matrix scattering theory (Mischenko and Travis, 1974), for the scattering angles used in the CAS. Each value of the F2BR is an average derived after calculating the scattering phase function assuming the spheroid passes through the beam in many different orientations.

The F2BR is not uniquely related to refractive index or aspect ratio, i.e. within certain size ranges and aspect ratios, the same F2BR could be measured for a spherical particle with a specific refractive index or an aspherical particle with a specific aspect ratio. Hence, in order to determine the refractive index or aspect ratio from a measured size and F2BR, look-up tables are used to find if a particle is unambiguously aspherical or not.
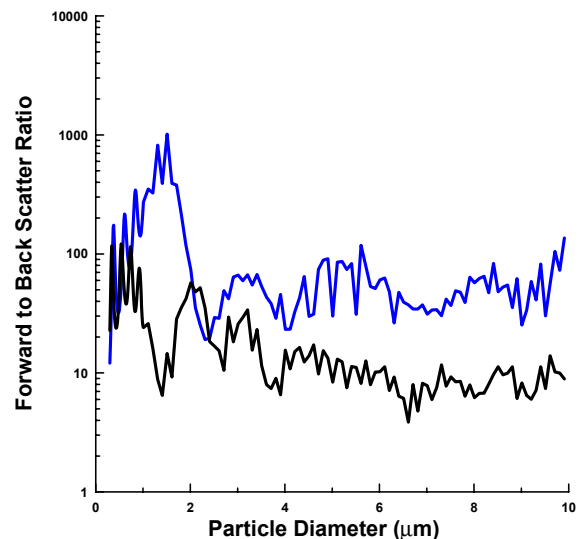

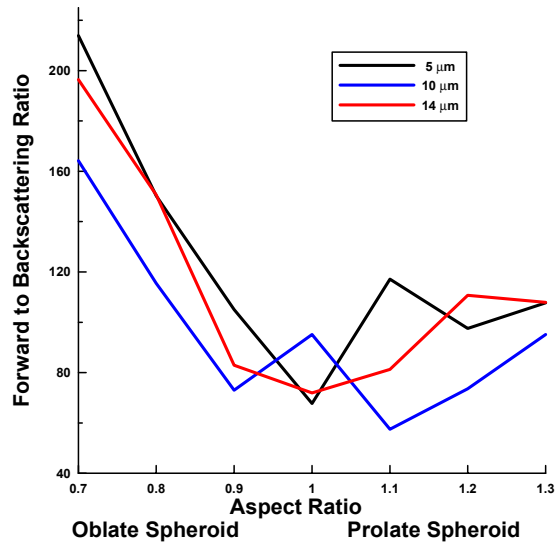Figure 3. Forward to back scattering ratio vs. particle diameter for two different refractive indices.

Figure 4. Forward to back scattering ratio vs. aspect ratio for 5, 10, and 14μm particles.
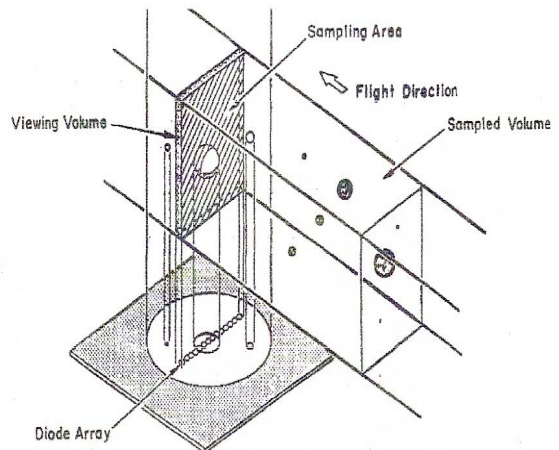

Figure 5. The fundamental measurement principle of the CIP is the imaging of the particles that pass through a collimated laser beam. Particles cast a shadow on a linear array of diodes and the processing electronics record the state of these diodes.

The utility of this capacity to measure the asphericity of small particles is that it allows us to distinguish between water and ice in a size range where shape is difficult to resolve with optical array probes that measure cloud particle images. Even with the Cloud Particle Imager (CPI), with its 2.3 μm resolution, the smallest particle whose shape can be resolved unambiguously is approximately 20 μm (*Korolev and Isaac*, 2003).

The cloud imaging probe (CIP) measures particles images by capturing the shadow of the particles that pass through a focused laser beam (Figure 5). A collimated laser beam from a 45-mW 0.685-μm wavelength diode laser is positioned on a linear array of 64 diodes. Each time the arrays moves a distance of 25 μm (the probe resolution), the on-off state of each of the diodes is recorded as the particle image moves across the array.

3. MEASUREMENT EXAMPLES

Figure 6 shows one of the contrail encounters on February 1, 2006. It illustrates the evolution of the concentration and size of the particles during four different passes of the aircraft through the contrail during five minute period. The increase in particle concentration is clearly seen as the contrail becomes older, at the same time we can see an increment in the amount of particles in the 10μm range. Moreover, over 90% of the particles are smaller than 2 μm.

Figure 7 shows four different frequency histograms of the particle diameters in the contrail, pertaining to each of the four passes through it. In these histograms we have a clearer image of the increase of the particle size in an older contrail. The growth process needs to be explored, i.e. whether aggregation, heterogeneous nucleation or diffusional growth is the principal mechanism for the rapid increase in particle concentration and size in the 10 μm range.

Figure 8 is a comparison of the microphysical properties of the subvisual cirrus and contrail particles. We see in the diameter histograms that both SVC and contrails have approximately the same frequency distribution by size; however, the SVC have somewhat more particles in the 10 – 20 μm range. The frequency

distribution of the refractive indices of particles in the cirrus and contrail were quite similar, having about 50% sphere-like particles with 20% of these particles with a refractive index similar to that of ice; i.e. in the range 1.31-1.33. It is also worth noticing the large fraction of particles in the SVC with refractive index of about 1.5. Further investigation is needed to see what other chemical constituents may be present in the ice particles. The principle difference between the subvisual cirrus and contrails is found in the spatial distribution of the particles. Those in the subvisual cirrus have a randomly uniform spatial distribution, indicated by the smooth, linear slope on the linear-log plot, whereas the particles in the contrail appeared more organized with non-random spacing that could indicate clustering.
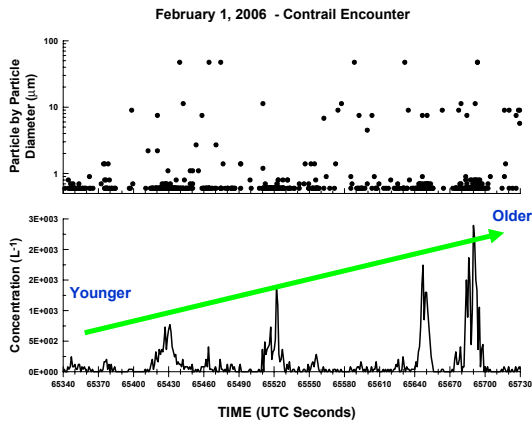

Figure 6. Evolution of particle diameters and concentration of particles during a contrail encounter on February 1, 2006.
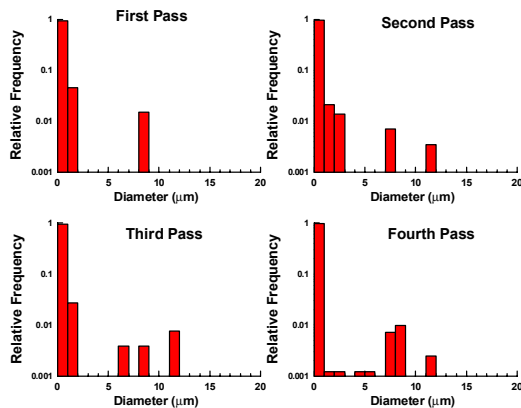

Figure 7. Frequency histograms of the contrail ice particles diameters during four different passes on February 1, 2006.
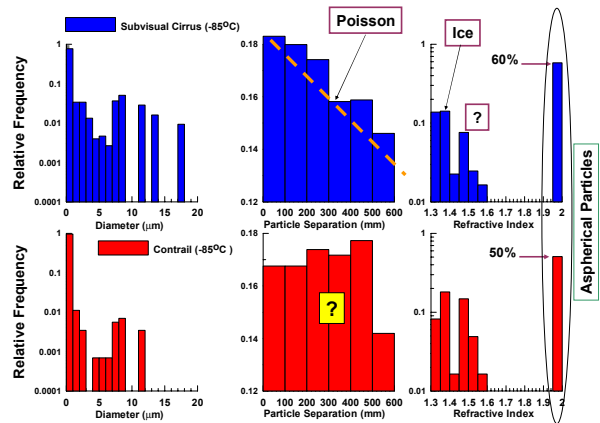

Figure 8. Comparison between three different microphysical properties of SVC and contrail particles: size distribution, spatial distribution, and frequency distribution of refractive indices.

4. SUMMARY

A comparison of the microphysical properties of the cirrus and contrails shows that the majority of particles were less than 40 μm and 50% of the particles were sphere-like. The principle difference between the subvisual cirrus and contrails was found in the spatial distribution of the particles. Those in the subvisual cirrus had randomly uniform spatial distributions whereas the particles in the contrail showed a preferred spacing, indicative of clustering or lack of mixing of newly formed particles with the environment.

Of the particles that were classified as sphere-like, approximately 20% had refractive indices representative of ice, i.e. in the range 1.31-1.33. The other sphere-like particles had average refractive indices of 1.40 and 1.54. The frequency distribution of the refractive indices of particles in the cirrus and contrail were quite similar.

Given that SVC near the tropical tropopause can modify the water vapor transfer to the lower stratosphere by simultaneously removing water vapor by sedimentation and lofting the affected air parcels through enhanced IR radiative heating of cloud particles (Jensen et al. 1996), a better understanding of the microphysical properties of SVC will help improve our comprehension of the climate impact of these clouds. Additionally, in situ measurements of the SVC microphysical properties, compared to measurements with remote sensors, will lead to improvements in how data from lidar and satellites are interpreted.

5. References:

Appleman, H., 1953. The formation of exhaust contrails by jet aircraft. *Bull. Amer. Metoer. Soc.* **34**, 14-20.

Baumgardner, D., J.E. Dye, B. Gandrud, K. Barr, K. Kelly, K.R. Chan, 1996: Refractive indices of aerosols in the upper troposphere and lower stratosphere, *Geophys. Res. Lett*, 23, 749-752.

Baumgardner, D., H. Jonsson, W. Dawson, D. O'Connor, R. Newton, 2002. The cloud, aerosol, and precipitation spectrometer: a new instrument for cloud investigations. *Atmos. Res.*, **59-60**, 251-264.

Baumgardner, D., H. Chepfer, G.B. Raga, G.L. Kok, 2005: The Shapes of Very Small Cirrus Particles Derived from In Situ Measurements, *Geophys. Res. Lett.,* **32**, L01806, doi:10.1029/2004GL021300, 2005

Chepfer, H., V. Noel, P. Minnis, D. Baumgardner, L. Nguyen, G. Raga, M.J. McGill, P. Yang, 2005**:** Particle Habit In Tropical Ice Clouds During CRYSTAL-FACE: Comparison of Two Remote Sensing Techniques With In Situ Observations, *J. Geophys. Res.*, VOL. **110**, D16204, doi:10.1029/2004JD005455, 2005

Goodman, J., R.F. Pueschel, E.J. Jensen, S. Verma, G.V. Ferry, S.D. Howard, S.A. Kinne, and D. Baumgardner, 1998. Shape and size of contrail ice particles. *Geophys. Res. Lett.*, **25**, 1327-1330

Heymsfield, A.J., 1986. Ice particles observed in a cirriform cloud at -83°C and implications for polar stratospheric clouds. *J. Atmos. Sci.,***43**, 851-855.

Jensen, E.J., O.B. Toon, L. Pfister, and H.B. Selkirk, 1996. Dehydration of the upper troposphere and lower stratosphere by subvisual cirrus clouds near the tropical tropopause, *Geophys. Res. Lett.,* **23**, 825-828.

Jensen, E.J., O.B. Toon, H. Selkirk, J.D. Spinhirne, and M.R. Schoeberl, 1996b. On the formation and persistence of subvisual cirrus clouds near the tropicap tropopause. *J. Geophys. Res.,***101**, 21361-21375.

Jensen, E.J., O.B. Toon, S. Kinne, G.W. Sachse, B.E. Anderson, K.R. Chan, C.H. Twohy, B. Gandrud, A. Heymsfield, and R.C. Miake-Lye, 1998b. Environmental conditions required for contrail formation and persistence. *J. Geophys. Res.*, **103**, 3929-3936

Joyce E. Penner, David Lister, David J. Griggs, David J. Dokken, Mack McFarland**,** Aviation and the Global Atmosphere: A Special Report of the Intergovernmental Panel on Climate Change, Cambridge University Press, 1999, Chapter 9.3.

Korolev, A. and G. Isaac, 2003: Roundness and aspect ratio of particles in ice clouds, *J. Atmos. Sci.*, 60, 1795-1808.

Mishchenko, M.I. and L. D. Travis, Capabilities and limitations of a current FORTRAN implementation of the T-matrix method for randomly oriented, rotationally symmetric scatterers, J. Quant. Spectrosc. Radiat. Transfer, 60, 309-324 (1998)

Pfister, L., H.B. Selkirk, E.J. Jensen, M.R. Schoeberl, O.B. Toon, E.V. Browell, W.B. Grant, B. Gary, M.J. Mahoney, T.V. Bui, and E. Hintsa, 2001. Aircraft observations of thin cirrus clouds near the tropical tropopause. *J. Geophys. Res.*, **106**, 9765-9786.

Sassen, K., and B.S. Cho, 1992. Subvisual/thin cirrus lidar dataset for satellite verification and climatology research. *J. Appl. Meteor.*, **31**, 1275-1285.

Schmidt, E., 1941. Die Entstehung von Eisnebel aus den Auspuffgasen von Flugmotoren. In *Schriften der Deutschen Akademie der Luftfahrtforschung*. Verlag R. Oldenbourg, München, Heft 44, pp. 1-15.

WMO, 1975. *International Cloud Atlas.* World Meteorological Organization, Geneva.